The Role of Attractive Interactions in Self-Diffusion

Scott D. Bembenek* and Grzegorz Szamel

Department of Chemistry, Colorado State University, Fort Collins, Colorado 80523-1872

Received: July 19, 2000; In Final Form: August 28, 2000

Recently, an alternative approach to self-diffusion in atomic liquids was proposed by one of us [Vergeles, M.; Szamel, G. *Chem. Phys.* **1999**, *110*, 3009]. This approach is applicable where the concept of binary collisions breaks down and the self-diffusion coefficient is small. Predictions from this method are in quantitative agreement with molecular dynamics (MD) simulations, over a broad range of densities and temperatures, for an atomic liquid interacting with a repulsive r^{-12} potential. Here we extend this approach to include attractive interactions; we study a liquid interacting with the Lennard-Jones (LJ) potential. Theoretical predictions are compared to MD simulations results. To clarify the role of attractive interactions, we compare LJ results with those obtained with the repulsive part of the LJ potential. Conclusions about the role of the attractive forces in self-diffusion are discussed.

I. Introduction

Often when one wants to describe chemically relevant processes, it is necessary to consider the dynamics of a single solute molecule interacting with its surrounding solvent. The simplest (and least chemically important) process of this type is self-diffusion. Other, more complicated (and, chemically, more important) examples include vibrational relaxation,[1−4] solvation dynamics,[5,6] and quadrupolar relaxation.[7,8]

A starting point for many theories of self-diffusion is kinetic theory. Its basic premise is to understand the macroscopic properties in terms of collisions between particles. The original kinetic equation was introduced by Boltzmann and still serves as a foundation for modern day theories. The Boltzmann equation fully accounts for the simplest class of collisions known as independent binary collisions.

The collision picture (more precisely, the *binary* collision picture) is applicable at low to moderate densities.[9,10] Its validity becomes questionable at higher densities. At lower densities the average time during which two particles interact (mean collision time) is much shorter than the average time between collisions (mean free time). It is this separation of time scales that allows us to consider dynamics as a sequence of (binary) collisions. At high densities the two time scales are comparable (in reality, both times are difficult to define unambiguously) and the binary collision picture cannot be valid.

To understand this quantitatively, we can consider the force autocorrelation function (FACF) of the total force acting on a tagged particle,

$$G_F(t) = \langle \sum_{i\neq 1} \mathbf{F}_{1i}(t) \cdot \sum_{i\neq 1} \mathbf{F}_{1i}(0) \rangle_{\mathrm{eq}} \tag{1}$$

and the "binary" contribution to the FACF, which is the autocorrelation function of the force on the tagged particle that is due to one other particle,

$$G_F^s(t) = \langle \sum_{i\neq 1} \mathbf{F}_{1i}(t) \cdot \mathbf{F}_{1i}(0) \rangle_{\mathrm{eq}} \tag{2}$$

It is clear that both force correlation functions will decay on the time scale of the mean collision time. On the other hand, the velocity autocorrelation function (VACF),

$$C_v(t) = \frac{\langle \mathbf{v}_1(t) \cdot \mathbf{v}_1(0) \rangle_{\mathrm{eq}}}{\langle \mathbf{v}_1 \cdot \mathbf{v}_1 \rangle_{\mathrm{eq}}} \tag{3}$$

will decay on the scale of the mean free time. Consequently, if the binary collision concept is valid for a given system, both force autocorrelation functions should decay much faster than VACF. Further, the characteristic decay time of the full force autocorrelation function and the binary contribution to it should be approximately equal. The latter condition is intuitively clear when one realizes that at low densities the major contribution to the force on a particle is primarily due to the contribution of, on the average, one other particle; in other words, the probability of finding several interacting particles is very low.

It has been shown by one of us[11] that while the mean free time and collision time are substantially different at low densities, they are comparable at liquid densities. Further, the full force autocorrelation function and the binary contribution to it are very different at liquid densities (although similar at low densities), indicating that the total force on a tagged particle is due to several neighboring particles comprising a solvation shell (cage). This illustrates that the binary collision picture is not warranted at liquid densities (except for the hard sphere fluid where the collision time is always zero).

It is often said[12] that there are two different, important effects in self-diffusion: "cage diffusion" and "vortex diffusion". They are responsible for the negative region and long-time tail appearing in the VACF, respectively. Both effects are supposed to be associated with so-called dynamically correlated collisions. It should be emphasized that these statements are based on an analysis of the dynamics of the hard sphere fluid. For a fluid interacting with a continuous potential at liquidlike densities the binary collision picture is invalid. The tagged particle, instead of undergoing dynamically correlated binary collisions, interacts with the whole solvation shell at the same time.

Recently, one of us has developed a new theory for self-diffusion that explicitly incorporates this fact. This theory has been applied to self-diffusion in an atomic liquid interacting through a repulsive r^{-12} potential.[11] It was also extended to the

10.1021/jp0025835 CCC: $19.00
Published on Web 10/24/2000

dynamic friction on a molecular bond.[13,14] Here we reconsider the atomic liquid. Specifically, we examine the role of the attractive forces in self-diffusion by comparing results obtained on a Lennard-Jones system to those obtained with only the repulsive part of the interaction potential.

In the next section we briefly recall the theoretical development that has already been presented in ref 11. Its application to the calculation of the self-diffusion coefficient D, the velocity autocorrelation function $C_v(t)$ and memory function $\zeta(t)$ is also outlined. In section III we describe the MD simulations used to calculate the equilibrium quantities needed by the theory. From the same simulations we also obtain dynamic quantities for comparison with theoretical results in section IV. Finally, a discussion on the possible role of the attractive interactions follows in section V.

II. Theory

The starting point of our theory is the introduction of the following set of distribution functions,

$$f_i(\mathbf{r}_1, \mathbf{v}_1, ..., \mathbf{r}_i, \mathbf{v}_i, \mathbf{F}; t) = \frac{(N-1)!}{(N-i)!}\int d\Gamma \prod_{k\le i}\delta(\mathbf{r}_k - \mathbf{R}_k)\,\delta(\mathbf{v}_k - \mathbf{V}_k)\,\delta(\mathbf{F} - \sum_{j\neq 1}\mathbf{F}_{1j})\,\rho_N(t) \quad (4)$$

where particle 1 has been tagged, Γ denotes positions and velocities of all the particles, $\Gamma \equiv (\mathbf{R}_1, ..., \mathbf{R}_N; \mathbf{V}_1, ..., \mathbf{V}_N)$, $\rho_N(t)$ is the time-dependent N-particle distribution function, $\mathbf{F}$ is the total force acting on the tagged particle, and $\mathbf{F}_{1j}$ is the force acting on the tagged particle from particle j. The probability at time t that the tagged particle is at $\mathbf{r}_1$ moving with velocity $\mathbf{v}_1$ while experiencing a force $\mathbf{F}$ is given by $f_1(\mathbf{r}_1, \mathbf{v}_1, \mathbf{F}; t)$. Similarly, the probability at time t that the tagged particle is at $\mathbf{r}_1$ moving with velocity $\mathbf{v}_1$ while experiencing a force $\mathbf{F}$ and another particle is at $\mathbf{r}_2$ moving with velocity $\mathbf{v}_2$ is given by $f_2(\mathbf{r}_1, \mathbf{v}_1, \mathbf{F}, \mathbf{r}_2, \mathbf{v}_2; t)$. The higher-order distributions have similar meanings.

It should be emphasized that the simplest distribution function used in a kinetic-theory type approach describes the state of the tagged particle only. In contrast, our f_1 describes the state of the tagged particle and also contains information about its immediate neighborhood. Therefore, our f_1 is a much more complicated object. In a sense, this is the price we pay for the failure of the binary collision picture!

The distributions f_i evolve in time according to an infinite hierarchy of equations similar to those in the BBGKY theory.[15] We use the first two of these equations and drop the three-particle terms in the second equation as our closure approximation and obtain the following approximate equation of motion for f_1 (see ref 11 for the details):

$$\frac{\partial y_1}{\partial t} = \hat{L}_0 y_1 + \frac{1}{f_1^{eq}}\int d2\ \mathbf{B}_{12}\cdot\frac{\partial}{\partial \mathbf{F}}\int_0^t d\tau\ e^{\hat{L}_2(t-\tau)} f_2^{eq}\mathbf{B}_{12}\cdot\frac{\partial y_1(\tau)}{\partial \mathbf{F}} \quad (5)$$

The first term on the right-hand side describes the oscillatory motion of the tagged particle in the cage formed by its neighbors. The second term on the right-hand side is a dissipation term responsible for the cage relaxation. In eq 5, $di \equiv d\mathbf{r}_i\, d\mathbf{v}_i$, $y_1 = f_1/f_1^{eq}$ and f_1^{eq} represents f_1 at equilibrium. The generalized one-particle equilibrium distribution f_1^{eq} is the product of the Maxwell velocity distribution and an equilibrium distribution of the total force acting on the particle 1. f_2^{eq} is the product of two Maxwell distributions and an equilibrium distribution function dependent on the force on particle 1, $\mathbf{F}$ and the distance between particle 1 and another particle of the fluid, $\mathbf{r}_{12}$.

The evolution operators, $\hat{L}_0$ and $\hat{L}_2$ are given by

$$\hat{L}_0 = -\mathbf{v}_1\cdot\frac{\partial}{\partial \mathbf{r}_1} - \mathbf{F}\cdot\frac{\partial}{\partial \mathbf{v}_1} + (\vec{\vec{\Omega}}^2\cdot\mathbf{v}_1)\cdot\frac{\partial}{\partial \mathbf{F}} \quad (6)$$

$$\hat{L}_2 = -\mathbf{v}_1\cdot\frac{\partial}{\partial \mathbf{r}_1} - \mathbf{F}\cdot\frac{\partial}{\partial \mathbf{v}_1} - \mathbf{v}_2\cdot\frac{\partial}{\partial \mathbf{r}_2} + \frac{\partial V(\mathbf{r}_{12})}{\partial \mathbf{r}_2}\cdot\frac{\partial}{\partial \mathbf{v}_2} + \mathbf{B}_{12}\cdot\frac{\partial}{\partial \mathbf{F}} \quad (7)$$

where

$$\mathbf{B}_{ij} = \frac{\partial}{\partial \mathbf{r}_i}\left((\mathbf{v}_i - \mathbf{v}_j)\cdot\frac{\partial V(\mathbf{r}_{ij})}{\partial \mathbf{r}_i}\right) \quad (8)$$

$$\vec{\vec{\Omega}}^2(\mathbf{F}) = \int d2\frac{f_2^{eq}}{f_1^{eq}}\frac{\partial^2 V(\mathbf{r}_{12})}{\partial \mathbf{r}_1 \partial \mathbf{r}_1} \quad (9)$$

The term $\vec{\vec{\Omega}}^2$ describes how the force changes when the tagged particle is moving and can be thought of as an *instantaneous* frequency tensor. It is analogous to the force constant matrix that is the basis of the INM approach.[16,17] However, $\vec{\vec{\Omega}}^2$ is a *local* quantity and describes the average curvature of the potential surface in the vicinity of the tagged particle whereas, the force constant matrix in the INM approach is describing the curvature of the many-body surface at a given time. The other difference is that $\vec{\vec{\Omega}}^2$ depends on $\mathbf{F}$, which means it will change in time, whereas the time dependence of the force constant matrix is usually ignored.

To calculate the velocity autocorrelation function (VACF) $C_v(t)$, we need to have a particular solution of eq 5, $\mathbf{j}(\mathbf{v}_1, \mathbf{F}; t)$, which at $t = 0$ is equal to $\mathbf{v}_1$. After finding $\mathbf{j}$, we take its first velocity moment to obtain VACF,

$$C_v(t) = \frac{1}{3k_BT}\int d1\ d\mathbf{F}\ f_1^{eq}(1, \mathbf{F})\mathbf{v}_1\cdot\mathbf{j}(\mathbf{v}_1, \mathbf{F}; t) \quad (10)$$

Clearly, eq 5 is a Boltzmann-like equation and, therefore, like its predecessor, is not directly solvable. To get explicit results, we use a moment expansion of $\mathbf{j}$,

$$\mathbf{j}(\mathbf{v}_1, \mathbf{F}; t) = C_v(t)\mathbf{v}_1 + B_v(t)\frac{\mathbf{F}}{\omega^2} + A_v(t)\frac{\vec{\vec{\Omega}}^2(\mathbf{F}) - \vec{\vec{I}}\omega^2}{\gamma\omega^4}\cdot\mathbf{v}_1 \quad (11)$$

ω^2 is the Einstein frequency,

$$\omega^2 = \frac{1}{3}\mathrm{Tr}\langle\vec{\vec{\Omega}}^2\rangle_F = \frac{n}{3}\int d\mathbf{r}\ g_2^{eq}(r)\nabla^2 V(r) \quad (12)$$

where n is the density, g_2^{eq} is the pair correlation function, and

$$\gamma = \frac{1}{3\omega^4}\langle\vec{\vec{\Omega}}^2 : \vec{\vec{\Omega}}^2\rangle_F - 1 \quad (13)$$

This moment expansion is motivated by the short time behavior of the VACF and is analogous to the Sonine polynomial expansion used in kinetic theory (see, e.g., ref 10, eq 4.3). The important difference between them being that here the basis functions depend on not just $\mathbf{v}_1$ but $\mathbf{F}$ as well. The time dependent coefficients in the expansion are interpreted as follows: $C_v(t)$ is the VACF, B_v is the force−velocity correlation function, and A_v is the correlation between $(\vec{\vec{\Omega}}^2(\mathbf{F}) - \vec{\vec{I}}\omega^2)\cdot\mathbf{v}_1$ and velocity.

Using ansatz (11), we can obtain a closed system of equations for A_v, B_v and C_v:

$$\dot{C}_v = B_v \tag{14}$$

$$\dot{B}_v = -\omega^2 C_v - A_v - \int_0^t \mathrm{d}\tau\, Z_0(\tau)\, B_v(t-\tau) - \int_0^t \mathrm{d}\tau\, Z_1(\tau)\, A_v(t-\tau) \tag{15}$$

$$\dot{A}_v = \gamma\omega^2 B_v - \int_0^t \mathrm{d}\tau\, Z_2(\tau)\, B_v(t-\tau) - \int_0^t \mathrm{d}\tau\, Z_3(\tau)\, A_v(t-\tau) \tag{16}$$

with the initial conditions

$$C_v(t=0) = 1 \qquad B_v(t=0) = 0 \qquad A_v(t=0) = 0 \tag{17}$$

The collision kernels Z_0, Z_1, Z_2, and Z_3 are given by the following formulas

$$Z_0(t) = \frac{1}{3k_B T\omega^2}\int \mathrm{d}1\ \mathrm{d}2\ \mathrm{d}\mathbf{F}\ \mathbf{B}_{12}\cdot \mathrm{e}^{\hat{L}_2 t} f_2^{\mathrm{eq}} \mathbf{B}_{12}$$

$$Z_1(t) = \frac{1}{3k_B T\gamma\omega^4}\int \mathrm{d}1\ \mathrm{d}2\ \mathrm{d}\mathbf{F}\ \mathbf{B}_{12}\cdot \mathrm{e}^{\hat{L}_2 t}\left(f_2^{\mathrm{eq}} \mathbf{B}_{12}\cdot\frac{\partial}{\partial \mathbf{F}}\right)(\vec{\Omega}^2\cdot\mathbf{v}_1)$$

$$Z_2(t) = \frac{1}{3k_B T\omega^2}\int \mathrm{d}1\ \mathrm{d}2\ \mathrm{d}\mathbf{F}\ \left(\mathbf{B}_{12}\cdot\frac{\partial}{\partial \mathbf{F}}\right)(\vec{\Omega}^2\cdot\mathbf{v}_1)\cdot \mathrm{e}^{\hat{L}_2 t} f_2^{\mathrm{eq}} \mathbf{B}_{12}$$

$$Z_3(t) = \frac{1}{3k_B T\gamma\omega^4}\int \mathrm{d}1\ \mathrm{d}2\ \mathrm{d}\mathbf{F}\ \left(\mathbf{B}_{12}\cdot\frac{\partial}{\partial \mathbf{F}}\right)(\vec{\Omega}^2\cdot\mathbf{v}_1)\cdot \mathrm{e}^{\hat{L}_2 t}\left(f_2^{\mathrm{eq}} \mathbf{B}_{12}\cdot\frac{\partial}{\partial \mathbf{F}}\right)(\vec{\Omega}^2\cdot\mathbf{v}_1)$$

To calculate these collision kernels, we need the equilibrium distribution $g_2^{\mathrm{eq}}(\mathbf{r}_1 - \mathbf{r}_2,\ \mathbf{F}) = f_2^{\mathrm{eq}}/(\phi_M(\mathbf{v}_1)\ \phi_M(\mathbf{v}_2))$. Since obtaining an exact analytical form for $g_2^{\mathrm{eq}}(\mathbf{r}_1 - \mathbf{r}_2, \mathbf{F})$ is not possible, we obtain this quantity from MD simulations. We would like to emphasize that the theory uses as input only *equilibrium* information about the liquid. Details of the calculation of the collision kernels has been previously given.[11] Once the collision kernels have been calculated, the equations of motion for A_v, B_v and C_v can be solved by using a Fourier−Laplace transform, $\tilde{f}(p) = \int_0^\infty \mathrm{d}t\ \mathrm{e}^{ipt} f(t)$. The transform of VACF is

$$\tilde{C}_v(p) = \left(\frac{\omega^2}{-ip + \tilde{Z}_0(p) + (1+\tilde{Z}_1(p))\dfrac{\gamma\omega^2 - \tilde{Z}_2(p)}{-ip + \tilde{Z}_3(p)}} - ip\right)^{-1} \tag{18}$$

VACF in the time domain is obtained by applying an inverse transform to eq 18. The Fourier−Laplace transform of the memory function $\tilde{\zeta}(p)$ is easily obtained from

$$\dot{C}_v(t) = -\int_0^t \mathrm{d}\tau\ \zeta(\tau) C_v(t-\tau) \tag{19}$$

as

$$\tilde{C}_v(p) = (\tilde{\zeta}(p) - ip)^{-1} \tag{20}$$

which given equation eq 18 becomes

$$\tilde{\zeta}(p) = \left(\frac{\omega^2}{-ip + \tilde{Z}_0(p) + (1+\tilde{Z}_1(p))\dfrac{\gamma\omega^2 - \tilde{Z}_2(p)}{-ip + \tilde{Z}_3(p)}}\right) \tag{21}$$

Finally, the self-diffusion coefficient is given by the following expression

$$D = k_B T \tilde{C}_v(0) = k_B T\left(\frac{\tilde{Z}_0(0)}{\omega^2} + (1+\tilde{Z}_1(0))\frac{\gamma - \tilde{Z}_2(0)/\omega^2}{\tilde{Z}_3(0)}\right) \tag{22}$$

III. Molecular Dynamics Simulations

All simulations were performed using a system of 500 particles. The Lennard-Jones (LJ) simulations actually utilize a slightly modified potential,

$$v(r) = 4\epsilon\left[\left(\frac{\sigma}{r}\right)^{12} - \left(\frac{\sigma}{r}\right)^{6}\right] + Ar^2 + B \tag{23}$$

where A and B are constant and chosen such that both the potential and the force are continuous at the potential cutoff, $r_{\mathrm{cut}} = 2.5\sigma$. All dimensionless quantities in this paper given as pure numbers should be understood as multiplied by an appropriate combination of MD units (σ, ϵ, and the particle mass, m). Conversion to argon values are more appropriately done using $\epsilon/k_B = 155.876$ K and $\sigma = 3.40$ Å[18] since the potential has been modified from its original form.

During a simulation run, the temperature was maintained by velocity scaling at every time step and periodic boundary conditions were applied. The equations of motion were integrated, with a time step of 0.0025τ or 0.005τ, depending on the temperature and density, using the velocity Verlet algorithm.[19,20] The system was initialized to a fcc lattice and heated to a temperature of 1.5 at a density of 0.40 and allowed to equilibrate for a total time of 1250τ (500 000 steps with a time step of 0.0025τ). Sets at different temperatures and densities were obtained using this original set and running it at the desired conditions for a total time of 1250τ. These sets were then run for another 1250τ to obtain the needed equilibrium averages: f_2^{eq}, which is used as input into the theory, and the self-diffusion coefficient, the VACF, and the memory function, which are compared to the theoretical predictions.

Values for self-diffusion and VACF are easily obtained from MD[19,20] but those for the memory function are more involved. We applied a discrete Fourier−Laplace transform to eq 19 and obtain an expression for the Fourier−Laplace transform of the memory function. This function is then inverted[23] to obtain the memory function in the time domain.

Results were also obtained for a system interacting with only the repulsive part of the potential (in eq 23) as defined by the WCA theory.[21] Since the potential has been modified from the original Lennard-Jones, the value of the minimum and the distance at which it occurs are slightly different from the usual values of 1.0 and $2^{1/6}\sigma$ respectively. Here, we find values of 0.9448 and 1.1228σ for the minimum value and distance, respectively. Simulations run with this potential were performed in a similar way to those previously described for the Lennard-Jones system.

IV. Results Theory vs MD

Theoretical results for the VACF, the self-diffusion coefficient and the memory function are compared to those obtained from

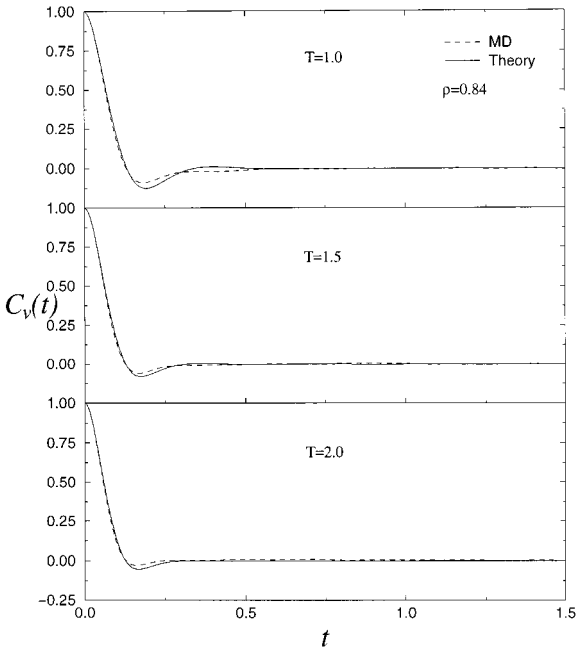

Figure 1. Velocity autocorrelation function $C_v(t)$ shown for temperatures $T = 1.0$, 1.5, 2.0 at constant density $\rho = 0.84$.

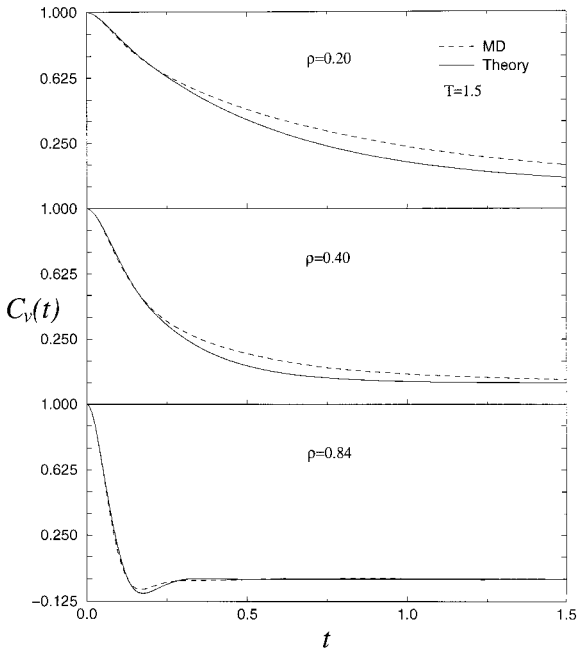

Figure 2. Velocity autocorrelation function $C_v(t)$ shown for densities $\rho = 0.20$, 0.40, 0.84 at constant temperature $T = 1.5$.

the same MD run that provides the equilibrium distribution f_2^{eq}. In Figure 1 we show the temperature dependence of the VACF at a constant density $\rho = 0.84$, while in Figure 2 we see the density dependence at a constant temperature $T = 1.5$. In both cases, we see quantitative agreement between the theory and simulation. In Figures 3 and 4 we present the temperature and density dependence of the memory function at a constant density $\rho = 0.84$ and temperature $T = 1.5$, respectively. Once again we see that the agreement is good, however, we note that our theory does not reproduce the long time features in the memory function that are usually attributed to dynamic correlations. In Figure 5 are self-diffusion coefficients as a function of temperature at constant densities $\rho = 0.70$, 0.84 along with a plot illustrating the density dependence at a constant temperature $T = 1.5$. Finally, Figure 6 compares the self-diffusion

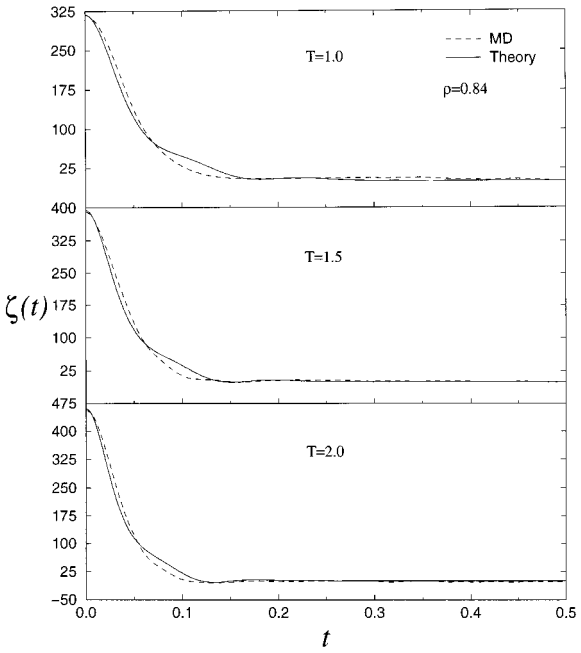

Figure 3. Memory function $\zeta(t)$ shown for temperatures $T = 1.0$, 1.5, 2.0 at constant density $\rho = 0.84$.

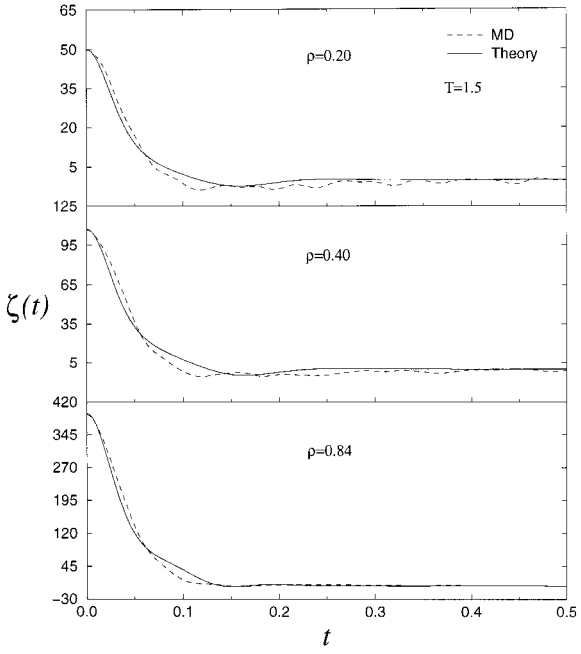

Figure 4. Memory function $\zeta(t)$ shown for densities $\rho = 0.20$, 0.40, 0.84 at constant temperature $T = 1.5$.

coefficients of the modified (see eq 23) Lennard-Jones and repulsive potentials. Theoretical calculations are in agreement with those obtained from MD, with the best results occurring at high densities in the case of the Lennard-Jones potential.

The main approximation used in deriving the current theory consists of neglecting terms, which in the low-density limit, are higher order in density than those retained in the Boltzmann equation. Therefore, we expect that at low density the theory should reproduce the Boltzmann theory. To show it explicitly, we would have to go beyond the simple three-moment expansion (11).

V. Discussion

The bottom plot in Figure 5 shows that the theory underestimates the self-diffusion coefficient at low densities for the

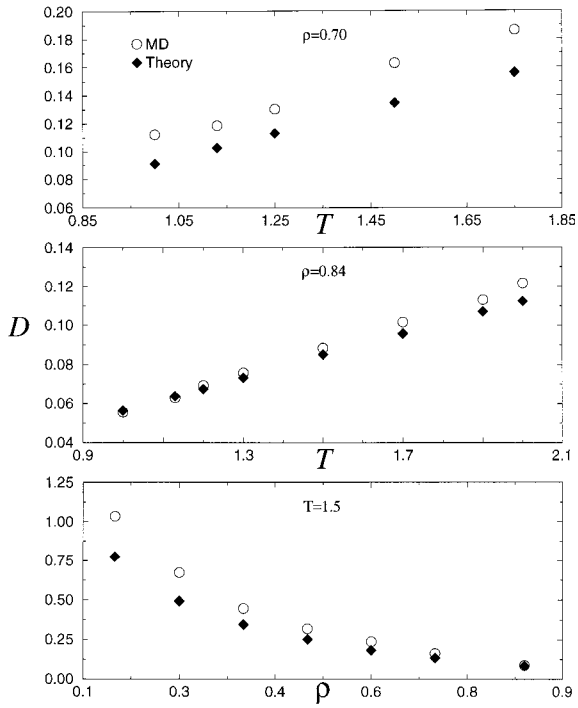

Figure 5. Self-diffusion coefficient for the modified Lennard-Jones potential is shown as a function of temperature for densities $\rho = 0.70$, 0.84 along with its density dependence at a constant temperature $T = 1.5$.

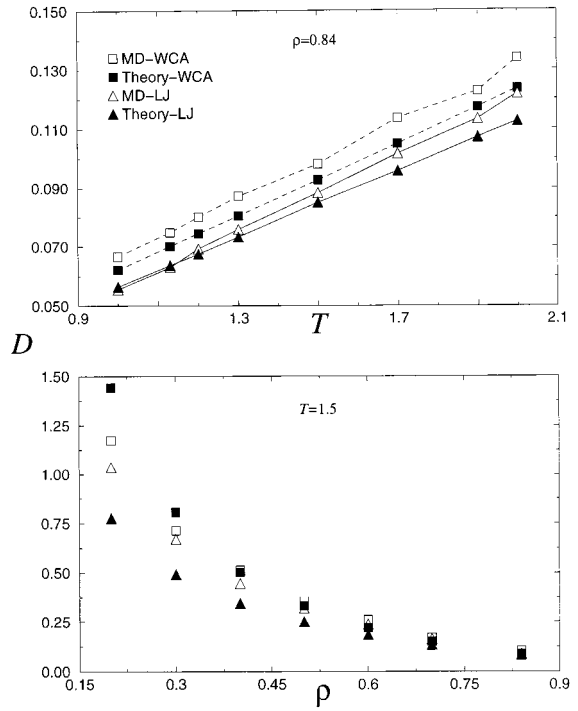

Figure 6. Self-diffusion coefficient for the modified Lennard-Jones and repulsive potentials are shown as a function of temperature for a density $\rho = 0.84$ along with their density dependence at a constant temperature $T = 1.5$. Dotted and solid lines, for the WCA and LJ potentials respectively, have been added to the top plot to provide clarity.

Lennard-Jones potential, whereas, in Figure 6 we see that the self-diffusion coefficient for the repulsive potential is well-described by the theory for all except the lowest density.

It should be noted here that a similar disagreement between theory and simulations for very low densities was found in an earlier application of the same method to self-diffusion in liquids interacting with a repulsive r^{-12} potential.[11] It was speculated there that the physical origin of the low-density failure of the theory is related to the breakdown of the expansion (11); in the low-density limit the large F tail of the force distribution, which describes the two-particle collisions, becomes more and more important and, therefore, the low moment expansion similar to (11) cannot be expected to work. We think that the same explanation applies in the present case. It should be emphasized that the approximations made in the derivation of the basic equation on which the whole theory is based, eq 5, consist in neglecting terms that are formally higher order in density than the terms that are retained. Therefore, we expect that eq 5 should become exact in the low-density limit. Search for a possible replacement of the moment expansion (11) that would be applicable in the low-density limit is left for future study.

The final and most important point is concerned with the role of attractive interactions in self-diffusion. Over thirty years ago Weeks, Chandler, and Anderson (WCA) established that the equilibrium structure of a liquid is primarily determined by the repulsive part of the potential.[21] Early on, this fact prompted Kushick and Berne[22] to consider the role of attractive forces in dynamics. They compared self-diffusion in a LJ fluid with that in a fluid interacting with only the repulsive part of the LJ potential (with the repulsive−attractive separation à la WCA). The disappointing finding was that although VACFs for both potentials were in qualitative agreement, the attractive part was found to contribute significantly to the transport coefficient; self-diffusion coefficients were found to be systematically larger for the system with the purely repulsive potential. Correspondingly, VACFs had negative regions that were less pronounced for the system with the purely repulsive potential.

This qualitative finding is well reproduced by our theory. As shown in Figure 6, self-diffusion coefficients for the repulsive part of the LJ potential (referred to as WCA in Figure 6) are larger than those for the full LJ potential. Also, the difference between VACFs was found to be qualitatively reproduced by the theory (not shown).

In conclusion, we can say that the theory correctly reproduces the influence of attractive interactions on self-diffusion. Therefore, it would be interesting to use it as a starting point for the development of a perturbative approach for the dynamical properties of liquids à la that proposed by WCA for the equilibrium properties.

Acknowledgment. G.S. is a Cottrell Scholar of Research Corp. This work was partially supported by NSF Grant No. CHE-9624596.

References and Notes

(1) Harris, C. B.; Smith, D. E.; Russel, D. J. *Chem Rev.* **1990**, *90*, 481.
(2) Berne, B. J.; Tuckerman, M. E.; Straub, J. E.; Bug, A. L. R. *J. Chem. Phys.* **1990** *93*, 5084.
(3) Goodyear, G.; Stratt, R. M. *J. Chem. Phys.* **1996**, *105*, 10050.
(4) Goodyear, G.; Larsen, R. E.; Stratt, R. M. *Phys. Rev. Lett.* **1996**, *76*, 243.
(5) Bagchi, B. *Annu. Rev. Phys.* **1989**, *40*, 115.
(6) Maroncelli, M. J. *J. Mol. Liq.* **1993**, *57*, 1.
(7) Hertz, H. G. *Ber. Bunsen-Ges. Phys. Chem.* **1973**, *77*, 531.
(8) Hynes, J. T.; Wolynes, P. G. *J. Chem. Phys.* **1981**, *75*, 395.
(9) Ranganathan, S. *Can. J. Phys.* **1983**, *61*, 1655.
(10) Leegwater, J. A. *J. Chem. Phys.* **1991**, *94*, 7402.
(11) Vergeles, M.; Szamel, G. *J. Chem. Phys.* **1999**, *110*, 3009.
(12) Cohen, E. G. D. *Am. J. Phys.* **1993**, *61*, 524.
(13) Vergeles, M.; Szamel, G. *J. Chem. Phys.* **1999**, *110*, 6827.
(14) Vergeles, M.; Szamel, G. *J. Chem. Phys.* **1999**, *111*, 4698.
(15) Résibois, P.; De Leener, M. *Classical Kinetic Theory of Fluids*; Wiley: New York, 1977.
(16) Bembenek, S. D.; Laird, B. B. *Phys. Rev. Lett.* **1995**, *74*, 936.

(17) Keyes, T. *J. Phys. Chem. A* **1997**, *101*, 2921.
(18) Bembenek, S. D.; Rice, B. M. *Mol. Phys.* **1999**, *97*, 1085.
(19) Allen, M. A.; Tildesley, D. J. *Computer Simulation of Liquids*; Oxford Science Press: Oxford, U.K., 1987.
(20) Frenkel, D.; Smit, B. *Understanding Molecular Simulations*; Academic Press: London, 1996.
(21) Weeks, J. D.; Chandler, D.; Andersen, H. C. *J. Chem. Phys.* **1971**, *54*, 5237.
(22) Kushick, J. N.; Berne, B. J. *J. Chem. Phys.* **1973**, *59*, 3732.
(23) Berne, B. J.; Harp, G. D. *Adv. Chem. Phys.* **1970**, *17*, 63.